Available online at www.sciencedirect.com
ScienceDirect
Journal of Photochemistry and Photobiology A: Chemistry 195 (2008) 284–294
Journal of Photochemistry and Photobiology A:Chemistry
www.elsevier.com/locate/jphotochem

Novel core-shell structured mesoporous titania microspheres: Preparation, characterization and excellent photocatalytic activity in phenol abatement

Jian-Hua Xu [a], Wei-Lin Dai [a,*], Jingxia Li [a], Yong Cao [a], Hexing Li [b], Kangnian Fan [a]

[a] *Department of Chemistry and Shanghai Key Laboratory of Molecular Catalysis and Innovative Materials, Fudan University, Shanghai 200433, PR China*
[b] *Department of Chemistry, Shanghai Normal University, Shanghai 200234, PR China*

Received 21 April 2007; received in revised form 1 September 2007; accepted 22 October 2007
Available online 1 November 2007

Abstract

Thermally stable mesoporous core-shell structured nanocrystallite titanium dioxide (TiO_2) microspheres were prepared by a novel hydro-alcohol thermal method. Anatase powders were synthesized under hydrothermal condition at 368 K from aqueous titania tetrachloride solution with the presence of urea and ammonium sulfate, then the samples were annealed at various temperatures before testing their photocatalytic activity. The morphology and microstructure characteristics of TiO_2 microspheres series were characterized by means of the specific surface area (BET), transmission electron microscopy (TEM), scanning electron microscopy (SEM), differential thermal analysis (DTA), photoluminescence spectra (PLS), X-ray photoelectron spectroscopy (XPS) and X-ray powder diffraction (XRD). The specific microsphere structures were maintained after a heat treatment at 973 K for 3 h, exhibiting a significant thermal stability. The photocatalytic activity was measured in a reactor with ultraviolet lamps. The catalysts show considerably high catalytic activity and recyclability during the photodegradation of phenol in aqueous suspension, the microsphere titania sample calcinated under 733 K for 3 h shows the best photocatalytic activity. The results obtained with this novel photocatalyst are compared with the behavior of the well-studied and widely used Degussa P25 TiO_2 under the same conditions.

Keywords: Titanium dioxide; Titanium tetrachloride; Microspheres; Photodegradation; Phenol

1. Introduction

In recent years, titania, as a popular inorganic material, has been widely used because of its various merits, such as optical and electronic properties, low cost, high photocatalytic activity, chemical stability and non-toxicity [1]. Proper control of these properties, especially morphology and crystallite structure, in the preparation of nanosized TiO_2, represents some of the key issues in this area. Because the crystalline state and structure of the support strongly affect the catalytic activity and selectivity, the design and selection of novel highly active catalysts places many requirements on the supports used. A considerable variety of nanostructured TiO_2 materials with different morphologies, including nanowires [2,3], nanorods [4,5], nanotubes [6–8], nanowhiskers [9,10], microspheres [11–14], foams [15,16] and films [17], have been successfully synthesized. In particular, the design and fabrication of spherical materials with hollow interiors has attracted considerable attention recently because of their potential applications as low-density capsules for controlled release of drugs, dyes and inks; development of artificial cells, protection of proteins, enzymes and DNA; and especially as supports of catalysts [18–22].

However, most of the systems reported for the formation of hollow spherical materials have been based on template-assisted processes involving the replication of organized reaction fields, such as emulsion foams [23–26], emulsion droplets and bicontinuous microemulsions [27–30], followed by removal of the template materials by calcination or solvent etching. All of the aforementioned methods generally require the use of surfactants or polymers that must be removed to create the hollow interiors.

* Corresponding author. Tel.: +86 21 55664678; fax: +86 21 65642978.
E-mail address: wldai@fudan.edu.cn (W.-L. Dai).

1010-6030/$ – see front matter © 2007 Elsevier B.V. All rights reserved.
doi:10.1016/j.jphotochem.2007.10.017

Such kind of treatment usually causes the microstructure transformation and accompanied with the phase transformation, severe sintering and/or growth of TiO_2 crystallites. Moreover, these materials are usually unstable and hence are limited in their potential applications, especially resulting in the severe decrease of activity in the photocatalytic reactions [31].

In a preliminary communication, we have reported a novel simple and nonsurfactant approach to synthesizing stable core-shell structured titania microspheres with hollow interiors [32]. During this process, the novel core-shell structured titania spheres are obtained after hydrothermal precipitation of titanium chloride ($TiCl_4$) with urea in ethanol/water solution containing ammonium sulfate ($(NH_4)_2SO_4$). The as-synthesized microspheres show no agglomeration or collapse of its special structure even after calcination at 873 K for 6 h. In addition, the core-shell titania microspheres have a mesoporous structure with a narrow pore size distribution in the nanometer range, and are also thermally stable and have much more surface area than other titania material previously reported. These novel characteristics all make possible its further application as a good catalyst support. For example, the heterogeneous WO_3/TiO_2 catalyst was synthesized by immobilization of tungsten oxide into the interior of the core-shell titania microspheres, which demonstrated much higher activity and selectivity in the oxidation of cyclopentene to glutaraldehyde with aqueous H_2O_2 under mild conditions [33].

To the best of our knowledge, there has been no report about the research of photocatalytic properties of the titania microsphere samples, though titanium dioxide is commonly considered as one of the most promising heterogeneous photocatalyst among the advanced oxidation processes. Among many semiconductor photocatalysts investigated, Degussa P25 TiO_2 is commonly used as a research standard. Considering the surface mediated character of heterogeneous photocatalytic processes, one of the main drawbacks of Degussa P25 TiO_2 is its relatively low specific surface area, thus limiting the number of available adsorption sites for pollutants to be degraded. Therefore, preparation of photocatalysts with higher specific surface area is a new research challenge. Most ultrafine TiO_2 nanocrystals exhibit high photocatalytic properties, however, two problems occur mainly in practical application. First, ultrafine nanocrystals will agglomerate into larger particles. Second, it is very hard to recover TiO_2 nanocrystals from water [34]. Mesoporous TiO_2 can partially solve such problems and have still comparatively high photocatalytic activity. In addition, considerable effort has been devoted to the study of reduction such problems [35–37].

In the present work, anatase TiO_2 powders was synthesized by hydrothermal method which has been applied to synthesize nanosized materials already [38–40], since products prepared by this method have well-crystalline phase, which benefits to thermal stability of the nanosized materials [41]. The samples have been characterized by X-ray diffractometry (XRD), specific surface area determinations, transmission electron microscopy (TEM) and scanning electron microscopy (SEM). The photodegradation of phenol was chosen as a probe reaction to measure the photocatalytic activity of different samples. The photocatalytic properties of commercial photocatalyst Degussa P25 was also presented with that of the nanocrystalline TiO_2 samples for the comparison purpose.

2. Experimental

2.1. Preparation of core-shell structured TiO_2 microspheres

Titanium tetrachloride ($TiCl_4$, analytical reagent grade) was used as titanium precursor. Commercially available reagents were obtained from Aldrich and used without further purification. The mesoporous core-shell structured titania microspheres was prepared by a hydro-alcohol thermal method with urea in ethanol/water solution in the presence of ammonium sulfate ($(NH_4)_2SO_4$). The preparation procedure was described in detail in our previous paper [32]. Certain amounts of ammonium sulfate and urea were dissolved in a dilute aqueous solution of titanium tetrachloride, then $TiCl_4$ was added to the above mixture and the operation was performed under ice-water bath to avoid a drastic hydrolysis of $TiCl_4$ in water at room temperature. After that, ethanol was added into the solution. The molar composition of $TiCl_4$: H_2O: EtOH:$((NH_4)_2SO_4)$:$CO(NH_2)_2$ was 1:86:24:1:46. After stirring for 2–4 h, a transparent solution was obtained. The mixture was transferred into an autoclave

Table 1
Textural and structural properties of TiO_2-MS samples calcined at different temperatures

Sample	Calcination temperature (K)	Surface area[a] ($m^2\ g^{-1}$)	Pore volume[a] ($cm^3\ g^{-1}$)	Crystallite phase[b] (%)	Crystallite size[c] (nm)
TiO_2-MS-AS	R.T.	334	0.40	A-100	A-4.2
TiO_2-MS-523	523	210	0.31	A-100	A-5.4
TiO_2-MS-673	673	125	0.22	A-100	A-8.8
TiO_2-MS-703	703	115	0.19	A-100	A-9.2
TiO_2-MS-733	733	81	0.15	A-100	A-11
TiO_2-MS-763	763	67	0.13	A-100	A-13
TiO_2-MS-793	793	24	0.06	A-100	A-23
TiO_2-MS-823	823	18	0.05	A-100	A-26
TiO_2-MS-973	973	~1	0.01	A-95/R-5	A-30/R-36
TiO_2-MS-1123	1123	~0	~0	R-100	R-36
Degussa P25	–	55	0.16	A-77/R-23	A-21/R-24

[a] BET surface area, average pore volume of the TiO_2-MS samples estimated from nitrogen adsorption.
[b] Ratio of phase of titania based on XRD data, where A and R represent the anatase and rutile phases, respectively.
[c] Average size of titania crystallites estimated from Scherrer equation.

of 200 mL capacity which was heated and maintained at 368 K for 5 h, and then allowed to cool to ambient temperature. The resulted slurry was filtered, twice washed with distilled water and subsequently washed carefully three times with absolute ethanol followed by vacuum drying at 373 K. Finally, the dried titania sample was calcined in a muffle furnace at certain temperatures for 3 h with the rate of 10 K min^{-1} in order to get the accurate phase transition temperature.

Ten new samples, including the as-prepared precipitate and nine calcined samples denoted as TiO_2-MS-AS, TiO_2-MS-523, TiO_2-MS-673, TiO_2-MS-703, TiO_2-MS-733, TiO_2-MS-763, TiO_2-MS-793, TiO_2-MS-823, TiO_2-MS-973 and TiO_2-MS-1123 were obtained (see Table 1).

2.2. Characterizations

XRD patterns of TiO_2-MS samples (2θ ranges from 20 to 70°) were recorded at room temperature with scanning speed of 2° min^{-1} using Cu Kα radiation ($\lambda = 0.154$ nm) from a 40 kV X-ray source (Bruker D8 advance) and diffracted beam monochromator, operated at 40 mA. The Scherrer equation was applied to estimate the average crystallite sizes of TiO_2 samples: $d = 0.89\lambda/B(2\theta)\cos\theta$, where $B(2\theta)$ is the width of the XRD peak at half peak-height in radian, λ is the wavelength of the X-ray in nanometer, θ is the angle between the incident and diffracted beams in degree and d is the average crystallite size of the powder sample in nanometer. The content of anatase in TiO_2 powder was calculated as follows [42]: $X_A(\%) = I_A/(I_A + 1.265I_R) \times 100$, where X_A is the content of the anatase phase, I_A and I_R are the peak intensities of anatase (1 0 1) and rutile (1 1 0), obtained from X-ray diffraction patterns, respectively.

Specific surface areas of TiO_2 samples were measured by nitrogen adsorption at 77 K (Micromeritics Tristar ASAP 3000) using Brunauer–Emmett–Teller (BET) method. The pore size distributions (average pore diameter and mean pore volume) were measured from the N_2 desorption isotherm using the cylindrical pore model (BJH method). Transmission electron micrographs were obtained using a JEOL 2011 microscope operating at accelerating voltage of 200 kV. The samples for electron microscopy were prepared by dispersing the powder in ethanol and applying a drop of very dilute suspension on copper grids. The suspensions were dried by slow evaporation at ambient temperature. Scanning electron micrographs were obtained using Philips XL 30 electron microscope. The samples were deposited on a sample holder with a piece of adhesive carbon tape and were then sputtered with a thin film of gold. Simultaneous thermal gravimetric (TG) and differential thermal analysis (DTA) measurements were performed between room temperature and 1273 K on a Perkin-Elmer 7 series thermal analyzer, using Al_2O_3 as a reference. Samples were heated at a rate of 10 K min^{-1} under a dynamic dry air atmosphere of 50 mL min^{-1}. For each experiment, 10–15 mg of sample was used. The UV light absorption and excitation were investigated by photoluminescence spectra (PLS, Varian Cary-Eclipse 500). X-ray photoelectron spectroscopy (XPS) measurements were performed on a PHI 5000C ESCA System with Mg Kα source at 14.0 kV and 25 mA, respectively. All the binding energies were referenced to the C1s peak at 284.6 eV of the surface adventitious carbon.

2.3. Adsorption and degradation of phenol

The phenol photodecomposition was conducted in a quartz reactor equipped with four black light blue fluorescent lamps which emit the light with the wavelength maximum at 365 nm of ultraviolet radiation with 8 W power for each one. The reaction system was placed in a self-constructed photoreactor which consists of a quartz tube (diameter 20 mm, length 250 mm) placed in the middle of the lamp bracket. In each experiment, the catalyst of 0.050 g was placed into 50 mL of phenol solution with the initial concentration of 0.060 g L^{-1} (6.3×10^{-4} mol L^{-1}) and the initial pH of 7.0, respectively. The reaction solution was sonicated for 20 min with a sonicator to obtain a homogeneous suspension. Phenol was adsorbed on the catalyst surface without UV irradiation for about 60 min to achieve the adsorption/desorption equilibrium established. During all experiments, the photoreactor was continuously purged with air at a flow rate of 100 mL min^{-1} to guarantee sufficient O_2 concentration in the reaction medium. After saturation of adsorption into catalysts, 3 mL of the prepared suspension was taken as a blank probe before irradiation and, after filtration by a dialyzer with the pore of 2 μm of the catalyst, for the UV–vis analysis. After that, the quartz tube was put into the photoreactor and the UV lamps were switched on in order to start the process of phenol decomposition. Measured irradiation power of UV rays inside reactor was about 1.8 mW cm^{-2}. In every 0.5 h, several milliliters of solution was sampled from the reaction mixture through a membrane filter in order to measure the phenol concentration in the same way as the blank probe. The concentration of phenol was calculated from the height of peak at 270 nm in UV–vis spectra (Shimadzu, UV-2450) by using calibration curve. The kinetic analysis was understood in terms of modified (for solid–liquid reactions) Langmuir–Hinshewood kinetic treatment. The corresponding kinetic curve of the standard photocatalyst TiO_2 P25 (Degussa) is included for comparison purpose. In cycling evaluation of titania samples, the reaction tube was placed softly for about 15 min until the catalyst was almost completely descended by gravity, then the reaction solution was removed and the photocatalyst was reused without further treatment. The sampling and detecting of the phenol concentration during recycling photodecomposition was the same as the former.

3. Results

3.1. X-ray diffraction

The crystal structure of TiO_2 depends on the temperature of heat treatment. It is commonly considered that the anatase phase of TiO_2 shows better photocatalytic activity than the rutile one. As-prepared sample without calcination as shown in Fig. 1(a) shows polycrystalline anatase phase. When the calcination temperature increases, the peak width and the intensity of anatase phase at $2\theta = 25.3°$ become more strong and sharp, indicating the formation of larger crystallite size and higher crystallinity

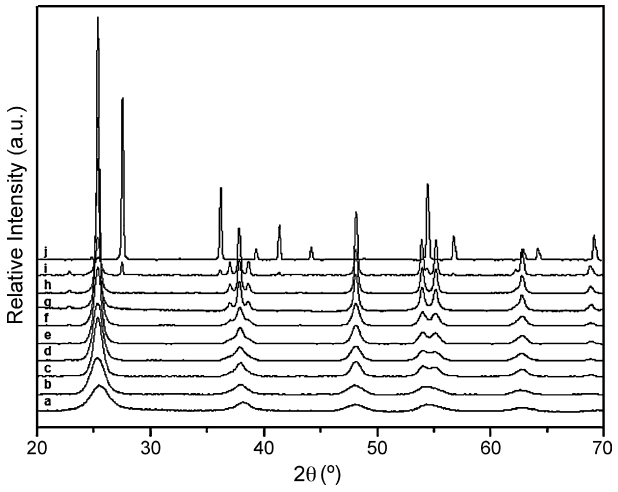

Fig. 1. X-ray diffraction patterns of TiO_2 samples. (a) As-prepared sample; (b) heated for 3 h at 523 K; (c) 673 K; (d) 703 K; (e) 733 K; (f) 763 K; (g) 793 K; (h) 823 K; (i) 973 K; (j) 1123 K.

by increasing the calcination temperature. Anatase-type TiO_2 could be obtained from not only the as-prepared sample but also those samples even heated up to 823 K for 3 h, during which no rutile-type TiO_2 was observed (see Fig. 1(a)–(h)). While the catalyst was calcined under 973 K, the phase transformation was started and small amount of rutile phase was observed in the titania sample. Our attention was focused on the inspection of the temperature below 973 K, where the TiO_2 samples keep their anatase phase and demonstrate higher photocatalytic activity. The result reveals that the present preparation is unique in producing anatase TiO_2 sample with considerably highly resistant to the phase transformation to rutile. The characteristic parts of XRD patterns of the as-prepared anatase TiO_2 and the samples calcined at 523, 673, 703, 733, 763, 793, 823, 973 and 1123 K were shown in Table 1. Powder XRD was used for crystal phase identification and the crystallite size of each phase present. The anatase (1 0 1) peak at $2\theta = 25.3^\circ$ and the rutile (1 1 0) peak at $2\theta = 27.6^\circ$ were analyzed using the formula in order to estimate the anatase–rutile ratio of TiO_2 samples: $X_R = (1 + 0.8 I_A/I_R)^{-1}$, where X_R is the weight fraction of rutile in the powders and I_A and I_R are the XRD peak intensities of the anatase and rutile phases, respectively.

The XRD pattern of the powder heated at 973 K shows the anatase (1 0 1) and the emerging peak of rutile (1 1 0), indicating that the sample TiO_2-MS-973 (Fig. 1(i)) is a mixture of anatase and rutile. Calcination at 973 K for 3 h resulted in obvious change in the intensity of both peaks. The intensity of the rutile phase peak increased while that of anatase one decreased. The TiO_2-MS-973 sample contains 95% of anatase and 5% of rutile and exhibits sharp XRD lines with a few signs of broadening. When the temperature of thermal treatment was risen to 1123 K, all of the anatase TiO_2 transformed to rutile phase (Fig. 1(j)). The average size of crystallites was calculated from the peak half-width B, using the Scherrer equation [43], $d = k\lambda/B(2\theta)\cos\theta$, where k is a shape factor of the particle (it equals to 1 if a spherical shape is assumed), λ and θ are the wavelength and the incident angle of the X-rays and B is the full width half maximum (FWHM) of the 2θ peak, respectively. The peak width was measured at half of the maximum intensity. The estimation shows that the mean crystallite size of the initial anatase TiO_2 individual particles (TiO_2-MS-AS) was about 4.2 nm, supposing that the broadening of peak is due to the size effect. Calcination is usually accompanied with crystal growth [44]. The crystallite size of each sample is presented in Table 1. From the data obtained above we can see that both anatase and rutile crystallite size are increased after calcination at overall temperature interval.

3.2. Particle morphology

It is believed that the urea precipitation method leads (under the reaction conditions used) to colloid anatase nanoparticles assembled into rather big (about 1–2 μm) porous spherical clusters (see Fig. 2) [45]. Fig. 2(a)–(f) shows the SEM micrographs of the TiO_2-MS-AS, TiO_2-MS-673, TiO_2-MS-733, TiO_2-MS-823, TiO_2-MS-973 and TiO_2-MS-1123 for each sample dried or annealed for 3 h at corresponding temperatures. Fig. 2(g) and (h) shows TiO_2-MS-733 recycled for 1 and 10 times after the photoreaction of degradation of phenol, respectively.

The SEM image of the as-prepared TiO_2-MS anatase sample (Fig. 2(a)) reveals that the titania powder consists of core-shell structured spherical particles. The size of spherical TiO_2 sample was comparatively uniformly sized. The diameter of the single dispersed microspheres was mostly within 2–3 μm. According to the inset SEM images, we can see the microsphere was in unique core-shell structure, the thickness of the shell was about 100 nm and a 300 nm interval was found between the core and shell layer. When the calcination temperature increases, the shape of these spherical particles remains unchanged after the thermal treatment process even the microspheres are calcined at 973 K for 3 h. In addition, the morphology of TiO_2-MS samples will not change while it was recycled in the reaction for 10 times (see Fig. 2(g) and (h)). Structural alterations in the material (*i.e.* growth of anatase nanocrystals, anatase to rutile transformation, growth of rutile nanocrystals and changes of porosity) take place inside of these spherical particles. Dramatically, significant sintering and morphology transformation between these spherical particles occurred when the sample was heated at 1123 K for 3 h (see Fig. 2(f)), while the microspheres were shattered and tremendously shrinked to irregular particles.

The insets of the SEM images, based on the TEM results (see Fig. 3(a) and (b)), indicate these spherical particles were consist of primary nanosized anatase crystallites. With the temperature of the thermal treatment goes up, the surface of the spheres become more and more granulate, denoting the incensement of the titania nanocrystallites, which was consistent well with the XRD result.

TEM image of the TiO_2-MS-AS was shown in Fig. 3(a). It was seen that the TiO_2 samples were composed of nanosized crystallites with clear core-shell structured microsphere morphology. The electron diffraction measurement of the selected area (Fig. 3(a), inset) demonstrated clear diffraction lines representative of anatase, namely, (1 0 1), (2 0 0), (0 0 4) and (2 1 1), indicating that the sample was in well-crystallized anatase phase and it was also confirmed by the result of X-ray diffraction.

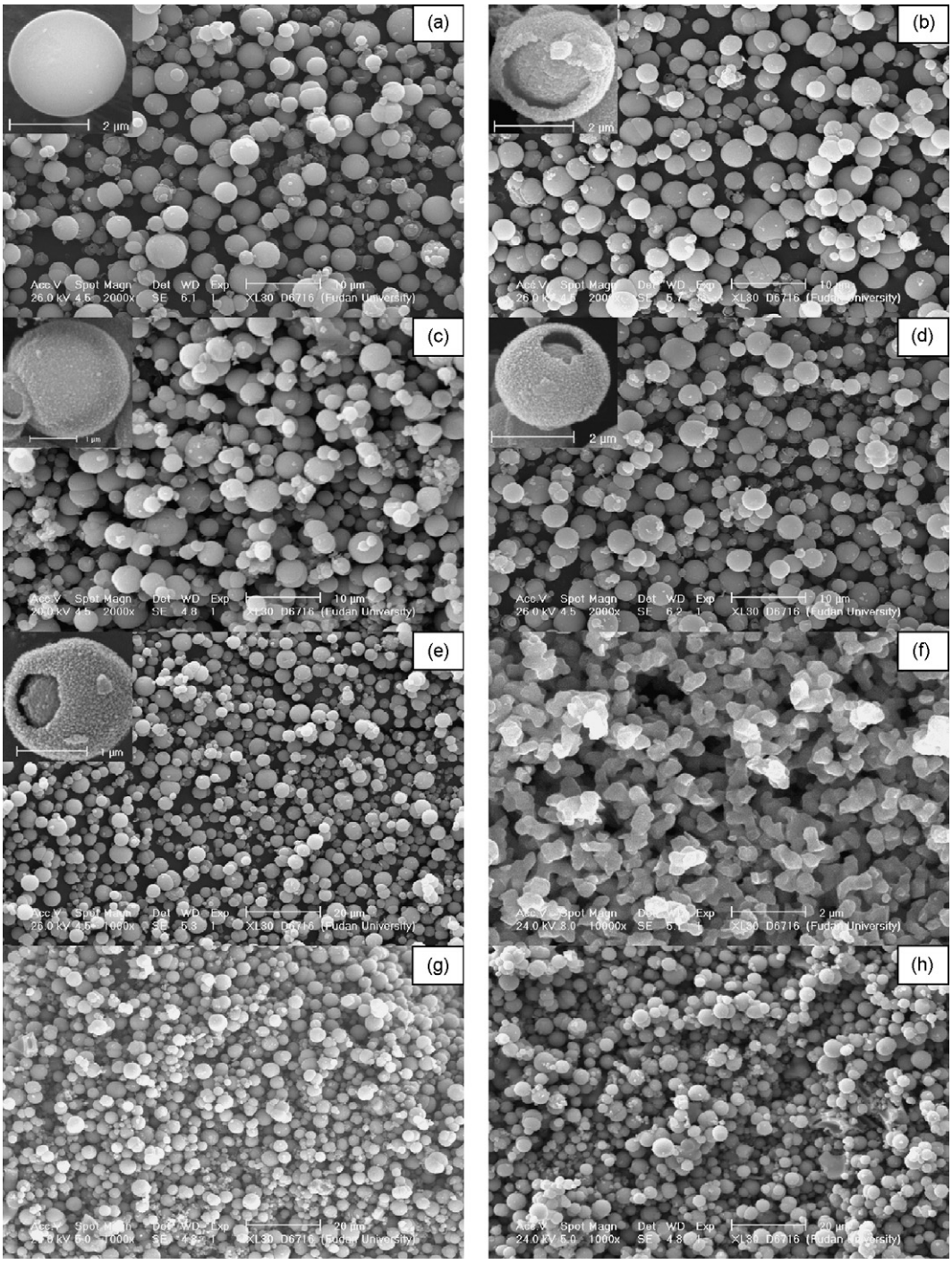

Fig. 2. SEM micrographs of TiO_2-MS samples. (a) As-prepared; (b) heated for 3 h at 673 K; (c) 733 K; (d) 823 K; (e) 973 K; (f) 1123 K; (g) sample after photoreaction; (h) after photoreaction for 10 times.

Fig. 3(b) gives the image of TiO_2-MS-733, and no significant size or morphology change of this catalyst was observed, while the thin shell, interior spacing and central core can be clearly recognized. High resolution TEM (Fig. 3(b), inset) confirms that the microspheres was consisted of single anatase crystallites, the microstructure diameter and crystalline size by TEM of the TiO_2-MS samples dried/calcined at various temperatures were found comparable with the characterization result of SEM and XRD, respectively.

3.3. The specific surface area, pore size and pore volume

The present preparation method can lead to the formation of well-defined mesoporous phases in the core-shell structured titania microspheres. The specific surface area of the samples is measured using the BET method by N_2 adsorption and desorption at 77 K. Table 1 shows the physicochemical properties of TiO_2-MS samples dried or calcined at temperatures ranging from ambient temperature to 1123 K. The as-prepared

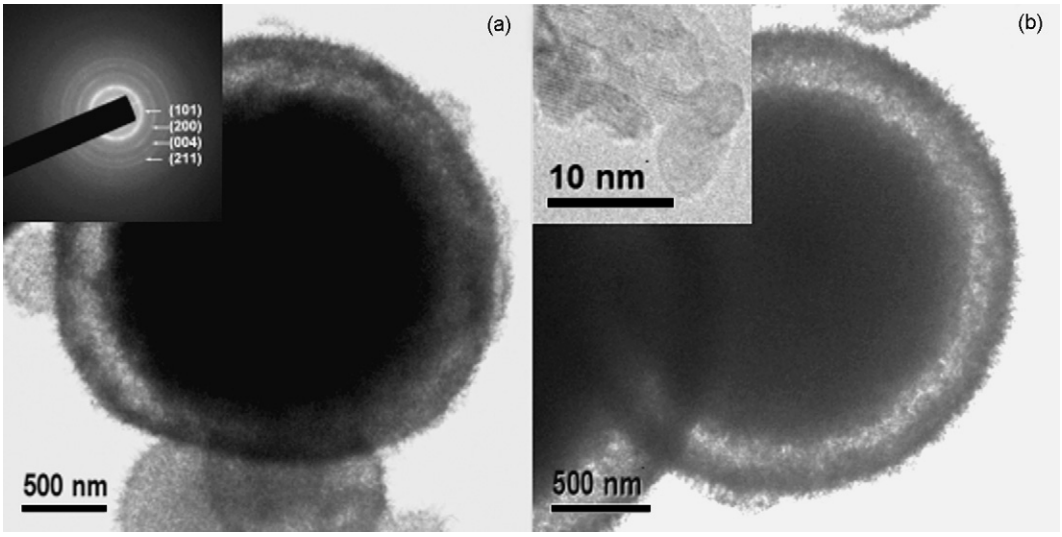

Fig. 3. TEM images and the HRTEM images or SAED images (inset) of TiO_2-MS samples. (a) TiO_2-MS-AS and (b) TiO_2-MS-733.

sample (*i.e.* TiO_2-MS-AS) showed a specific surface area of 334 $m^2\,g^{-1}$, about six times larger than Degussa P25, even larger than TiO_2 nanotube [46]. While the sample was calcined at 673 or 733 K for 3 h, it still presented a high specific surface area of 125 or 81 $m^2\,g^{-1}$, respectively, still much larger than P25. In this range of thermal treatment temperature, the titania microspheres show best photoactivity in decomposition of aqueous phenol solution, even significantly higher than P25. With a high calcination temperature, the surface area of the samples were seen to reduce to 18 $m^2\,g^{-1}$ (TiO_2-MS-823) and 1 $m^2\,g^{-1}$ (TiO_2-MS-973) when the calcination temperature was further increased to 823 and 973 K, respectively. The variation of the sample pore volume followed the same trend of the surface area with the calcination temperature. The average pore volume of TiO_2-MS-AS sample was 0.40 $cm^3\,g^{-1}$ while commercial P25 was only 0.16 $cm^3\,g^{-1}$, and the calcined TiO_2 sample (TiO_2-MS-733) gave almost the same result as P25. With the increase of calcination temperature, the pore volume becomes smaller, accompanied with the decrease of photoactivity.

Fig. 4(a) and (b) shows the nitrogen adsorption–desorption isotherm of TiO_2-MS-AS and TiO_2-MS-733, respectively. The type IV-like isotherms with inflection of nitrogen-adsorbed volume at $P/P_0 = 0.45$ (type H_2 hysteresis loop) indicated the presence of well-developed mesoporosity in the microspheric samples. Moreover, the inset in Fig. 4(a) and (b) shows the pore size distribution plots calculated using the BJH equation from the adsorption branch of the isotherm. The pore size distribution measurements indicate that the spherical titania sample have pronounced mesoporosity of narrow pore size distribution with average pore diameter around 3.5 and 5 nm. The mesoporous structure was maintained after 733 K calcination, but the pore volume was lessened and the average pore size was gently increased. It is known that commercial Degussa P25 shows no mesoporosity, which might be one reason why the present core-shell structured titania shows much higher photoactivity than that of P25.

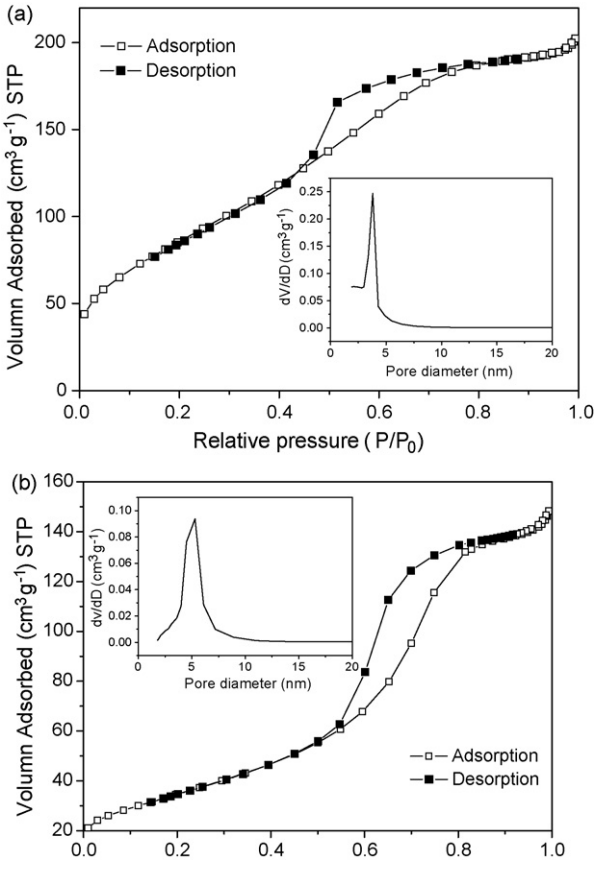

Fig. 4. Nitrogen adsorption/desorption isotherms and the corresponding pore size distribution (inset) of (a) TiO_2-MS-AS and (b) TiO_2-MS-733.

3.4. Thermal analysis

Fig. 5(a) and (b) shows thermogravimetry–differential thermal analysis (TG–DTA) curves of the TiO_2-MS-AS and TiO_2-MS-733 samples in flowing air (50 mL min^{-1}) at the heating rate of 10 K min^{-1}. The TG curve can be divided into three

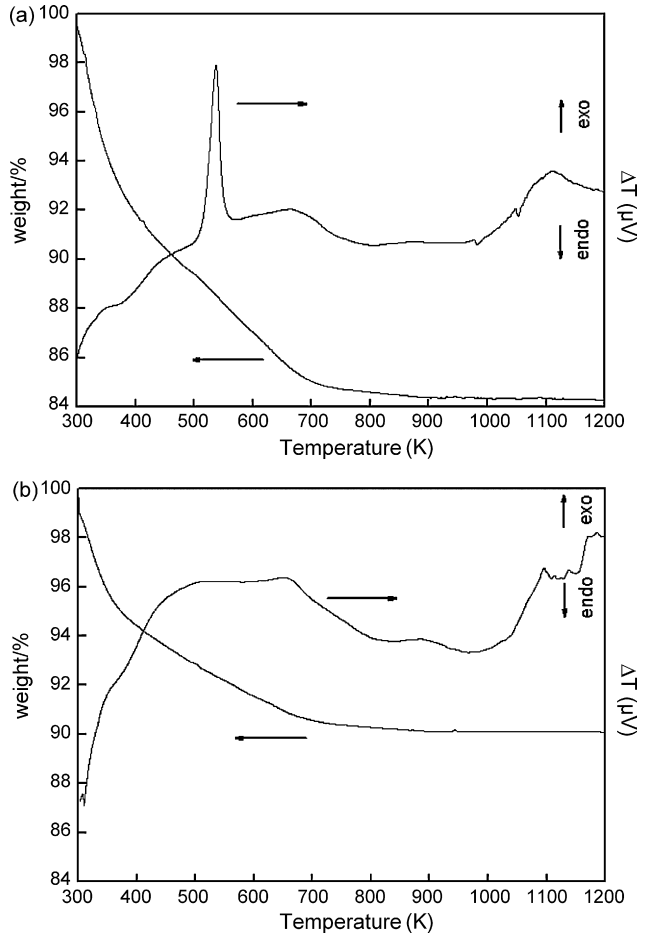

Fig. 5. Thermal analysis (TG/DTA) curves of TiO_2-MS-AS and TiO_2-MS-733 at 10 K min^{-1} ramp under 20 mL min^{-1} air flow.

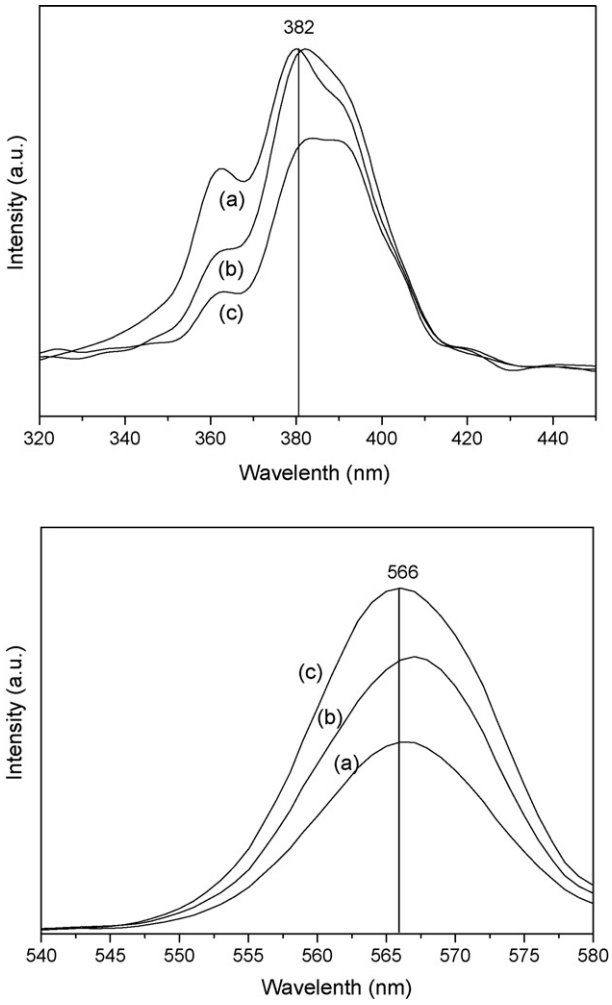

Fig. 6. Photoluminescent spectra (PLS) of (a) TiO_2-MS-733, (b) TiO_2-MS-AS and (c) P25.

stages. The first stage is from room temperature to 473 K, over which the mass loss of 10% was observed, which was caused by the elimination of the volatile composition such as water and ethanol from the catalyst. The second stage is from 523 to 573 K, where the mass loss is about 5%. This can be assigned to the elimination of carbonaceous residues. The third stage is from 773 to 1273 K, where the mass loss is firstly about 1% and then the mass remains constant, indicating the loss of surface hydroxyl groups.

The DTA curve shows a broad endothermic peak at about 373 K due to the desorption of adsorbed water/ethanol for the TiO_2-MS samples. The DTA curve of Fig. 5(a) giving an aculeate exothermic peak at 523 to 573 K indicated the decomposition of residual organic compounds of the catalyst, while Fig. 5(b) shows no such peak. The broad exothermic peak at about 773 K gives the evidence of the crystallization of anatase phase. The as-prepared sample contained some of the remaining amorphous titania, which converted to anatase phase at about 773 K, and this process was exothermic. The peak at 1023 to 1273 K indicates the phase transformation from anatase to rutile of the titania samples, which is an exothermic peak without mass loss. The result from thermal analysis was in well agreement with that from XRD results.

3.5. The photoluminescence and the X-ray photoelectron spectroscopy

The photoluminescence spectra (PLS) demonstrated that the samples of (a) TiO_2-MS-733, (b) TiO_2-MS-AS and (c) P25 exhibited typical PLS peaks, as shown in Fig. 6. The PLS demonstrated that all of the three samples exhibited two PLS peaks at 382 and 560 nm. According to the reference, the peak at about 382 nm could be attributed to an emission peak from band edge free excitation, mainly corresponding to the oxygen vacancies and/or defects of the TiO_2 particles [47]. The stronger emission peak at 382 nm implied the presence of more oxygen vacancies and/or defects. We could find that the peak of TiO_2-MS-733 was stronger than the other samples, indicated the oxygen vacancies and/or defects was more than that of P25 and TiO_2-MS-AS. This led to less recombination of photo-induced electrons and holes, so the quantum yield and photocatalytic activity of TiO_2-MS-733 sample was the best. TiO_2 microspheres, especially TiO_2-MS-733, have weaker emission peak than P25, owing to their unique core-shell structure that make the photo-induced electrons and holes easier to separate. Liu et al. [48] suggested

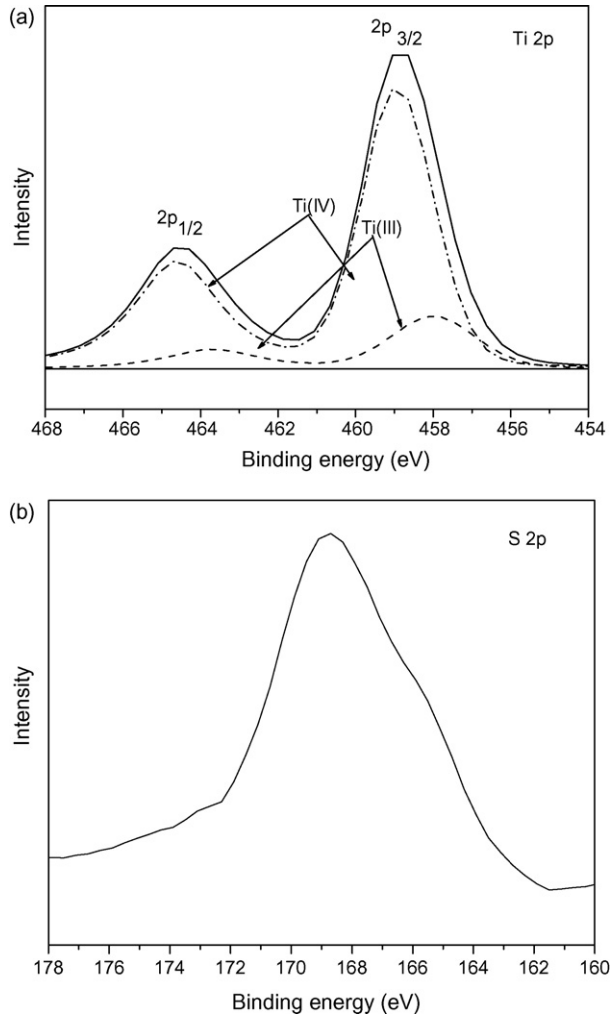

Fig. 7. XPS spectra of the (a) Ti 2p and (b) S 2p for TiO_2-MS-733. The sulfur percentage of which is ca. 2.0% (atomic ratio).

that the signal at about 560 nm was possibly related to the ability of TiO_2 sample for absorbing ultraviolet light and that the weaker photoluminescence intensity demonstrated that TiO_2-MS-733 may absorb more UV lights. The strong ability of absorbing ultraviolet and high quantum yield make the TiO_2-MS-733 sample an active and promising photocatalyst in degrading phenol.

The results from XPS of TiO_2-MS-733 proved that the materials contain some residual sulfate on the surface of TiO_2 particles, as shown in Fig. 7. The sulfur percentage of which is ca. 2.0% (atomic ratio). The peak of S 2p around 169 eV related to S–O bond was assigned to the SO_4^{2-} ←ions adsorbed on the surface of TiO_2 powders [49]. As it has been previously reported, pre-treatment with sulfate of TiO_2-precursor and further calcination produces interesting stabilization of surface area and anatase phase at rather high temperature. According to the above XPS results, it can be inferred that S element might be in situ doped into TiO_2 during hydrolysis of $TiCl_4$ with ammonia, and the S element may come from ammonium sulfate. It is also observed that the XPS signal of Ti $2p_{3/2}$ can be fitted into two components, one located at 458.9 eV, attributed to Ti(IV) species and the other located at 458.0 eV, assigned to Ti(III) species [50,51].

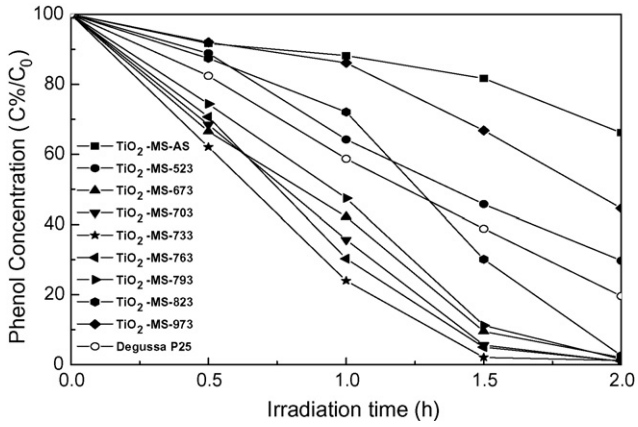

Fig. 8. Time courses of the photocatalytic decomposition of phenol on annealed TiO_2-MS samples and Degussa P25.

3.6. Photocatalytic activity of TiO_2 samples in photodegradation of phenol

The course of phenol photodecomposition using the catalyst TiO_2-MS series annealed at various temperatures was given in Fig. 8. Degussa P25 was used as the reference material for comparison purpose. As in the controlled experiment in which phenol is in TiO_2 suspensions in the dark or is illuminated with ultraviolet light in the absence of TiO_2 does not exhibit obvious photocatalytic activity (<5%). However, most of the samples demonstrate quite high photoactivity. It is interesting to find that the sample TiO_2-MS-733 exhibited the best photocatalytic efficiency on the degradation of phenol of all the tested TiO_2 samples and phenol was completely eliminated within 90 min. It is evident that the photoactivity of the sample calcined at proper temperature is superior to the standard photocatalyst Degussa P25. After annealing at temperatures of 973 K the activity decreased significantly, with the sample sintering and the starting of the phase transformation. When the catalyst was calcined at 1123 K with the phase completely changed to rutile and significant sintering occurred, almost no photoactivity was observed under this condition.

The TiO_2-MS samples can be easily separated from the reaction mixture directly by the removal of solvent based on simple gravity of the sample. After completing abatement of phenol, the purge of air was stopped and the reaction suspension was placed in darkness in order to get the catalyst come to settlement for about 15 min. The transparent solvent was poured and the catalyst was separated for the recycle of the reaction. Each cycle of the photocatalytic reaction was maintained for 90 min. Fig. 9 shows the results of the recycling results of TiO_2-MS-733 catalyst with different reaction cycles, the result of commercial P25 sample used for the first time was also listed. As shown, TiO_2-MS-733 gives nearly 90% abatement of phenol even after the tenth cycle while P25 only gives 60% for the first time, indicated the outstanding activity and recycling ability of the core-shell structured TiO_2 microspheres.

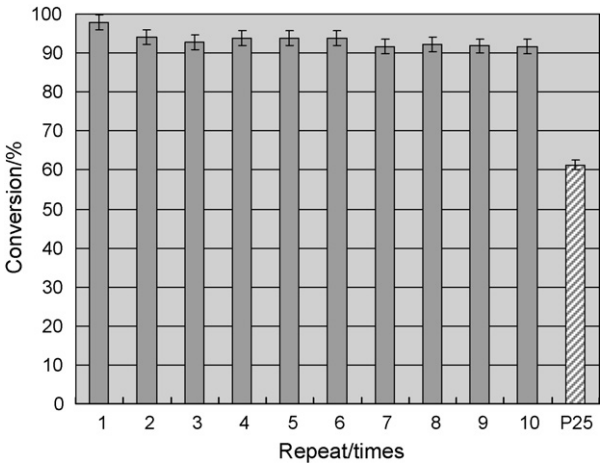

Fig. 9. Recycling results of TiO_2-MS-733 sample (Degussa P25 for comparison).

4. Discussion

The previous work shows that uniformly sized core-shell structured anatase titania microspheres are successfully synthesized by a simply alcohol-hydrothermal method (as-preparation) without any templates or shape-protectors. Although there are some reports on the synthesis of titania microspheres in the presence of organic templates [52,53] or without templates [54,55], no other references mentioned the template-free synthesis of core-shell structured titania microspheres. In the present work, no template is used for the synthesis and the formation of unique morphology anatase TiO_2 takes place during the alcohol-hydrothermal processing. This finding suggests that there should be another mechanism for the formation of TiO_2-MS samples different from the process with template existence. The formation of TiO_2-MS samples can be explained by the symmetric Ostwald Ripening in the fabrication process [56,57]. However, detailed explanation of such a mechanism is beyond the scope of the present work.

The TiO_2-MS samples take advantage of the absence of the template during the synthetic process, and the TiO_2-MS-AS sample without calcination can give comparatively high photocatalytic activity in degrading phenol while most of the hydrothermal process should be followed with the removal of the template by thermal, microwave or ultraviolet treatment, otherwise the carbonaceous residues would cap over the active sites of the photocatalyst. Usually, this kind of treatment of the titania samples accompanied with the increase of crystallization degree, sintering of the nanocrystallites and/or distinct decrease of specific surface area [58,59].

The titania microspheres show anatase phase without further thermal treatment and are comparatively highly thermally stable. Only little rutilization existed even after the TiO_2-MS sample was calcined at 973 K. Because the anatase phase was present itself, the samples would not undergo a phase transformation process from amorphous to anatase during the following moderately thermal treatment. In general, this kind of phase transformation is also harmful to keep high specific surface area, porosity and photoactivity [60]. Although there is still much debating on whether activity of a photocatalyst can be related to the catalyst surface area, since photocatalytic reactions are believed to proceed only on the illuminated surface. However, one could argue that adsorption on the catalyst surface would at least help to "concentrate" the reactant molecules for the photoreactions and the photos might be scattered between the nanosized TiO_2 particles. Also, photogenerated electrons and holes as well as the adsorbed molecules might be able to diffuse more or less at the catalyst surface, causing the photoreactions more easy to happen [31]. The core-shell structured titania microspheres with extremely high specific surface area may help this process more efficiently in the degradation of phenol.

The amount of adsorbed phenol on the catalysts is related to the surface area and micro-morphology of different catalysts, which can affect the activity of photocatalysts. TiO_2-MS can absorb more phenol than P25 owing to its large surface area, moreover, the crystallization degree of anatase and the core-shell structure of TiO_2 both influence their photodegradation activity of phenol. However, when compared with the activity test results, the absorption contributes little to the total activity (<5%) since the absorption of phenol under dark circumstance is a typical equilibrium process. Therefore, the amount of adsorbed phenol is not a crucial parameter to the present photocatalytic process although it is very important for the present TiO_2-MS-733 catalyst. In addition, there is a thin and porous shell covers each titania microsphere, the core-shell structure of TiO_2 composes a micro-reactor and phenol solution filled in the interspace. Within the micro-reactor, the relative consistency of photocatalyst is much more than the rest area, so the adsorbed phenol decomposes rapidly and exterior phenol supplies continuously to keep the concentration of both sides equal, which also speed up the reaction process.

This core-shell structure of the photocatalyst facilitates the degradation of phenol not only from above reasons but also from the optic consideration. As we are known, the photocatalytic efficiency is closely related to the width of the photocatalyst band gap and also to the amount of the photo-induced electrons and holes. The interspaces between the core and shell may inhibit the recombination of the photo-induced electrons and holes, since photo-induced electrons could be separated by the space. As proved by PLS spectra, the higher emission peaks of TiO_2-MS-733 and TiO_2-MS-AS were corresponded to the more oxygen vacancies and/or defects, thus, the quantum efficiency of the TiO_2 photocatalyst was enhanced, resulting in the higher photocatalytic activity.

As it has been previously reported, pre-treatment with sulfate of TiO_2-precursor and further calcination produces interesting stabilization of surface area and anatase phase at rather high temperature [61]. It is well established that adsorbed sulfate groups retain the anatase structure avoiding rutilization process, which is stated to be a topotactic transformation. In Ref. [62], information given by XRD and Raman spectroscopy supports this statement. On the other hand, in addition to the structural stabilization during calcination, acidification of TiO_2-precursor with sulfuric acid produces an increase of the adsorbed protons [63]. The excess of surface protons in the TS-precursor affects the

OH^-/H^+ equilibrium at the surface. The sulfate-modification resulted in the higher surface area and larger pore size as well as pore volume, which allowed more phenol molecules to be adsorbed on the catalyst surface, facilitating the phenol degradation. The sulfate-modification enhanced the crystallization degree of the anatase phase, which has been claimed to be favorable for the phenol degradation [64].

XPS investigation of binding energies and intensities of the surface elements provides information on the chemical states and relative quantities of the outermost surface compounds. It is observed that the XPS signal of Ti $2p_{3/2}$ can be fitted into two components, one located at 458.9 eV, attributed to Ti(IV) species and the other located at 458.0 eV, assigned to Ti(III) species. This indicates that there are two types of titanium oxide species on the surface of the core-shell structured titania spheres, with relative amounts of the Ti(IV) and Ti(III) species about 78.7 and 21.3%, respectively. According to Ref. [65], appropriate ratio of Ti(III) species in the TiO_2 samples can enhance the activity of the TiO_2 photocatalysts.

The TiO_2-MS samples present high photocatalytic activity as well as good recycling ability, and the unique single dispersed spherical sample showed not only regular morphology. In fact, comparably uniform microspheres with diameter of several microns could be easily separated from the reaction mixture and recycled for more than 10 times. During the cycling process, the catalytic activity keeps almost the same. This kind of catalyst was proved to be highly effective as photocatalyst and other heterogeneous catalysts, and it was further expected to be useful in other fields.

5. Conclusions

In summary, mesoporous core-shell structured TiO_2 microspheres with highly thermal stability and high surface area was prepared by a novel hydro-alcohol thermal route, which increases the thermal stability of the powders significantly. The TiO_2 microspheres with high specific surface areas exhibit considerably high activity in photocatalytic degradation of phenol. Moreover, the photocatalytic activity of TiO_2 microspheres increases with the calcination temperature at interval of 673–823 K due to the increase in the crystallization degree of the anatase phase. The sample calcined at 733 K (TiO_2-MS-733) gives the best photocatalytic activity and demonstrates to be far superior to that of the commercial Degussa P25 counterpart. The excellent recycling ability and its easy separation from the reaction mixture all make the core-shell structured TiO_2 microspheres a promising candidate in further industrial application.

Acknowledgements

We are grateful to the financial supports from the Major State Basic Resource Development Program (Grant no. 2003CB615807), NSFC (Project 20573024, 20407006) and the Natural Science Foundation of Shanghai Science & Technology Committee (06JC14004).

References

[1] M.R. Hoffmann, S.T. Martin, W.Y. Choi, D.W. Bahnemann, Chem. Rev. 95 (1995) 69.
[2] Y.X. Zhang, G.H. Li, Y.X. Jin, Y. Zhang, J. Zhang, L.D. Zhang, Chem. Phys. Lett. 365 (2002) 300.
[3] Y. Gao, Y.X. Ma, H.L. Li, Chem. J. Chin. Univ. Chin. 24 (2003) 1089.
[4] P.D. Cozzoli, A. Kornowski, H. Weller, J. Am. Chem. Soc. 125 (2003) 14539.
[5] Q. Huang, L. Gao, Chem. Lett. 32 (2003) 638.
[6] Z.R.R. Tian, J.A. Voigt, J. Liu, B. McKenzie, H.F. Xu, J. Am. Chem. Soc. 125 (2003) 12384.
[7] S.M. Liu, L.M. Gan, L.H. Liu, W.D. Zhang, H.C. Zeng, Chem. Mater. 14 (2002) 1391.
[8] X.H. Li, X.G. Zhang, H.L. Li, Chem. J. Chin. Univ. Chin. 22 (2001) 130.
[9] Y.C. Zhu, H.L. Li, Y. Koltypin, Y.R. Hacohen, A. Gedanken, Chem. Commun. (2001) 2616.
[10] G.L. Li, G.H. Wang, J.M. Hong, J. Mater. Res. 14 (1999) 3346.
[11] T. Nakashima, N. Kimizuka, J. Am. Chem. Soc. 125 (2003) 6386.
[12] B.L. Zhang, B.S. Chen, K.Y. Shi, S.J. He, X.D. Liu, Z.J. Du, K.L. Yang, Appl. Catal. B:Environ. 40 (2003) 253.
[13] M. Keshmiri, T. Troczynski, J. Non-Cryst. Solids 311 (2002) 89.
[14] L.Z. Wang, S. Tomura, M. Maeda, F. Ohashi, K. Inukai, M. Suzuki, Chem. Lett. (2000) 1414.
[15] I.M. Arabatzis, P. Falaras, Nano. Lett. 3 (2003) 249.
[16] A. Imhof, D.J. Pine, Adv. Mater. 11 (1999) 311.
[17] M.C. Carotta, M. Ferroni, V. Guidi, G. Martinelli, Adv. Mater. 11 (1999) 943.
[18] D.L. Wilcox Sr., M. Berg, T. Bernat, D. Kelleman, J.K. Cochran Jr., Hollow and Solid Spheres and Microspheres: Science and Technology Associated with their Fabrication and Application, MRS Proceedings, vol. 372, Materials Research Society, Pittsburgh, PA, 1994.
[19] E. Mathiowitz, J.S. Jacob, Y.S. Jong, G.P. Carino, D.E. Chickering, P. Chaturvedi, C.A. Santos, K. Vijayaraghavan, S. Montgomery, M. Bassett, C. Morrell, Nature 386 (1997) 410.
[20] H.Y. Huang, E.E. Remsen, T. Kowalewski, K.L. Wooley, J. Am. Chem. Soc. 121 (1999) 3805.
[21] Z.Z. Yang, Z.W. Niu, Y.F. Lu, Z.B. Hu, C.C. Han, Angew. Chem. Int. Ed. 42 (2003) 1943.
[22] R.F. Xu, X.X. Hu, W.K. Hu, P. Zhang, Abstr. Papers Amer. Chem. Soc. 226 (2003) U705.
[23] D. Walsh, S. Mann, Nature 377 (1995) 320.
[24] A. Imhof, D.J. Pine, Nature 389 (1997) 948.
[25] J. Jang, J.H. Oh, Adv. Mater. 15 (2003) 977.
[26] S.C. Gu, T. Kondo, E. Mine, D. Nagao, Y. Kobayashi, M. Konno, J. Colloid Interface Sci. 279 (2004) 281.
[27] D. Walsh, J.D. Hopwood, S. Mann, Science 264 (1994) 1576.
[28] M. Ohmori, E. Matijevic, J. Colloid Interface Sci. 150 (1992) 594.
[29] S.D. Sims, D. Walsh, S. Mann, Adv. Mater. 10 (1998) 151.
[30] D.S. Bae, D.J. Kim, K.S. Han, J.H. Adair, J. Ceram. Proc. Res. 3 (2002) 38.
[31] H. Wang, Y. Wu, B.Q. Xu, Appl. Catal. B:Environ. 59 (2005) 139.
[32] C.W. Guo, Y. Cao, S.H. Xie, W.L. Dai, K.N. Fan, Chem. Commun. (2003) 700.
[33] X.L. Yang, W.L. Dai, C.W. Guo, H. Chen, Y. Cao, H.X. Li, H.Y. He, K.N. Fan, J. Catal. 234 (2005) 438.
[34] D. Beydoun, R. Amal, G.K.C. Low, S. McEvoy, J. Phys. Chem. B 104 (2000) 4387.
[35] J.C. Yu, X.C. Wang, X.Z. Fu, Chem. Mater. 16 (2004) 1523.
[36] H.Y. Zhu, J.A. Orthman, J.Y. Li, J.C. Zhao, G.J. Churchman, E.F. Vansant, Chem. Mater. 14 (2002) 5037.
[37] Q.H. Zhang, L. Gao, S. Zheng, Chem. Lett. (2001) 1124.
[38] H. Kominami, J. Kato, Y. Takada, Y. Doushi, B. Ohtani, S. Nishimoto, M. Inoue, T. Inui, Y. Kera, Catal. Lett. 46 (1997) 235.
[39] H. Kominami, S. Murakami, Y. Kera, B. Ohtani, Catal. Lett. 56 (1998) 125.
[40] Q.W. Chen, Y.T. Qian, Z.Y. Chen, G.I. Zhou, Y.H. Zhang, Mater. Lett. 22 (1995) 77.

[41] J.F. Zhu, W. Zheng, H.E. Bin, J.L. Zhang, M. Anpo, J. Mol. Catal. A:Chem. 216 (2004) 35.
[42] R.A. Spurr, H. Myers, Anal. Chem. 29 (1957) 760.
[43] F.J. Pocock, J.F. Stewart, J. Eng. Power Trans. ASME 85 (1963) 33.
[44] G.V. Vasilenko, V.I. Zarembo, A.A. Slobodov, Russ. J. Appl. Chem. 70 (1997) 1498.
[45] S. Bakardjieva, J. Subrt, V. Stengl, M.J. Dianez, M.J. Sayagues, Appl. Catal. B:Environ. 58 (2005) 193.
[46] T. Kasuga, M. Hiramatsu, A. Hoson, T. Sekino, K. Niihara, Adv. Mater. 11 (1999) 1307.
[47] H. Yamashita, Y. Ichihashi, M. Anpo, J. Phys. Chem. 100 (1996) 16041.
[48] H. Liu, H.J. Wu, F.X. Sun, Y.L. Yao, M. Wu, W.Z. Li, Chin. J. Mol. Catal. 15 (2001) 47.
[49] Q. Zhang, J. Wang, S. YIN, T. Sato, F. Saito, J. Am. Ceram. Soc. 87 (2004) 1161.
[50] C.D. Wagner, W.M. Riggs, L.E. Davis, J.F. Moudler, G.E. Muilenberg (Eds.), Handbook of X-Ray Photoelectron Spectroscopy, Perkin-Elmer, 1992, p. 73.
[51] J. Pouilleau, D. Devilliers, H. Groult, P. Marcus, J. Mater. Sci. 32 (1997) 5645.
[52] X.M. Sun, J.F. Liu, Y.D. Li, Chem-Eur. J. 12 (2006) 2039.
[53] C.R. Han, W.L. Lu, X.Y. Wu, X. Fu, Z.S. Hu, J. Inorg. Mater. 20 (2005) 1409.
[54] X.M. Wang, P. Xiao, J. Mater. Res. 20 (2005) 796.
[55] L.J. Zhang, M.X. Wan, Y. Wei, Synth. Met. 151 (2005) 1.
[56] B. Liu, H.C. Zeng, Small 1 (2005) 566.
[57] H.G. Yang, H.C. Zeng, J. Phys. Chem. B 108 (2004) 3492.
[58] J. Ovenstone, J. Mater. Sci. 36 (2001) 1325.
[59] J.G. Yu, H.G. Yu, B. Cheng, X.J. Zhao, J.C. Yu, W.K. Ho, J. Phys. Chem. B 107 (2003) 13871.
[60] D. Grosso, G. Soler-Illia, E.L. Crepaldi, F. Cagnol, C. Sinturel, A. Bourgeois, A. Brunet-Bruneau, H. Amenitsch, P.A. Albouy, C. Sanchez, Chem. Mater. 15 (2003) 4562.
[61] G. Colon, M.C. Hidalgo, J.A. Navio, Appl. Catal. B:Environ. 45 (2003) 39.
[62] G. Colon, M.C. Hidalgo, G. Munuera, I. Ferino, M.G. Cutrufello, J.A. Navio, Appl. Catal. B:Environ. 63 (2006) 45.
[63] R.A. Young, P. Desai, Arch. Nauki. Mater. 10 (1989) 71.
[64] S. Yamazaki, N. Fujinaga, K. Araki, Appl. Catal. A: Gen. 210 (2003) 97.
[65] H.M. Liu, W.S. Yang, Y. Ma, J.N. Yao, Appl. Catal. A: Gen. 299 (2006) 218.